

Defect Tolerant Monolayer Transition Metal Dichalcogenides

Mohnish Pandey,¹ Filip A. Rasmussen,¹ Korina Kuhar,¹ Thomas Olsen,¹ Karsten W. Jacobsen,¹ and Kristian S. Thygesen^{1,2}

¹*Center for Atomic-scale Materials Design,
Department of Physics, Technical University of Denmark,
DK - 2800 Kongens Lyngby, Denmark*

²*Center for Nanostructured Graphene (CNG),
Department of Physics, Technical University of Denmark,
DK - 2800 Kongens Lyngby, Denmark**

(Dated: April 13, 2016)

Abstract

Localized electronic states formed inside the band gap of a semiconductor due to crystal defects can be detrimental to the material's opto-electronic properties. Semiconductors with lower tendency to form defect induced deep gap states are termed defect tolerant. Here we provide a systematic first-principles investigation of defect tolerance in 29 monolayer transition metal dichalcogenides (TMDs) of interest for nano-scale optoelectronics. We find that the TMDs based on group VI and X metals form deep gap states upon creation of a chalcogen (S, Se, Te) vacancy while the TMDs based on group IV metals form only shallow defect levels and are thus predicted to be defect tolerant. Interestingly, all the defect sensitive TMDs have valence and conduction bands with very similar orbital composition. This indicates a bonding/anti-bonding nature of the gap which in turn suggests that dangling bonds will fall inside the gap. These ideas are made quantitative by introducing a descriptor that measures the degree of similarity of the conduction and valence band manifolds. Finally, the study is generalized to non-polar nanoribbons of the TMDs where we find that only the defect sensitive materials form edge states within the band gap.

* thygesen@fysik.dtu.dk

Single layers of semi-conducting transition metal dichalcogenides (TMDs) are presently attracting much attention due to their unique opto-electronic properties which include direct-indirect band gap transitions[1–4], valley selective spin-orbit interactions,[5, 6] high charge carrier mobilities,[7–9] and strong light-matter interactions arising from large oscillator strengths and tightly bound excitons.[10, 11] Another attractive feature of the two-dimensional (2D) materials is that their electronic properties can be readily tuned e.g. by applying strain [12], electrostatic gating [13, 14], or by van der Waals heterostructure engineering[15–17]. In parallel with this development new 2D materials are continuously being discovered. For example, monolayers and multilayers of MoTe₂, NbSe₂, NiTe₂, TaS₂, TaSe₂, TiS₂, WS₂, WSe₂, ZrS₂ have recently been synthesized or isolated by exfoliation.[18].

One of the main performance limiting factors of opto-electronics devices such as photo detectors, light emitting diodes, solar cells, and field effect transistors, is the presence of crystal defects in the active semiconductor material. Such defects can act as local scattering centers which reduce the mobility of charge carriers and enhance non-radiative recombination of photo-excited electron-hole pairs. The effectiveness of a defect to scatter charge carriers, trap excitons and induce recombination between electrons and holes depends crucially on the way the defect modifies the electronic structure around the band edges; in particular whether or not it introduces localized states inside the band gap (deep gap states). On the other hand, defect states lying close, i.e. on the order of $k_B T$, to the conduction or valence band edges (shallow defect states) might enhance the charge carrier concentration and thereby the conductivity.[19] Depending on the extent of localization of a defect state it might affect the mobility as well. The materials where defects introduce deep gap states are termed defect sensitive, while the materials where no or only shallow levels appear are called defect tolerant.

There have been several experimental [20, 21] and theoretical [22] studies of defects and their influence on the electronic properties of few-layer MoS₂ - the most well studied of the TMDs. These studies indicate that S vacancies are the most common type of defects and that they lead to the formation of localized states inside the band gap. The sulphur vacancies are believed to be the main reason for the low mobility observed in back gated field effect transistors based on chemical vapour deposition (CVD) grown MoS₂, which is usually 1-2 orders of magnitude lower than the theoretical limit set by phonon scattering [7, 8]. In contrast, mobilities very close to the theoretical limit were recently measured in van der

Waals heterostructure devices where a high quality mechanically exfoliated MoS₂ monolayer was encapsulated into hexagonal boron nitride and contacted by graphene electrodes [9]. Defect-induced deep gap states are also responsible for the ultrafast non-radiative recombination of photo-excited excitons in MoS₂ which limits the quantum efficiency of CVD grown TMDs to <0.01.[23–25] Indeed, it was recently demonstrated that chemical passivation of the dangling bonds around the S vacancies in MoS₂ increases the photoluminescence quantum efficiency to almost unity.[26, 27] However, defects and impurity doping can also be used constructively. For example, p-type conductivity in MoS₂, which is otherwise naturally n-doped, has been recently explored via Niobium doping which introduces shallow acceptor levels near the valence band edge. [28, 29]. Defect states in monolayer WSe₂, [30] and hBN [31] have recently been shown to act as single photon emitters with exciting opportunities for quantum technology. Engineering of the chemical activity of monolayer MoS₂ for the hydrogen evolution reaction was recently demonstrated via tuning the concentration of sulfur vacancies. [32]

In this Letter, we systematically explore the tolerance of monolayer TMDs to chalcogen vacancies. Using ab-initio methods we calculate band structures of 29 monolayer semiconducting TMDs with and without chalcogen vacancies. The compounds have been selected from a 2D materials database which contains different electronic properties calculated from first-principles DFT and GW methods. [33]The correlation between the tendency of TMDs to form deep gap states and the orbital character of the valence and conduction band is established via a simple descriptor, the normalized orbital overlap (NOO), which is calculated from the projected density of states of the pristine system. We find that deep gap states are introduced for all the TMDs based on group VI and group X metals valence and conduction bands have similar orbital character (NOO close to 1) while no states or only shallow states are introduced for the other materials (NOO significantly less than 1). Additionally, we explore nanoribbons of all the TMDs and find that cleaving of the monolayer along a non-polar direction of the defect tolerant TMDs induces only shallow states in the band gap as opposed to the nanoribbons of defect sensitive TMDs which all have metallic edge states.

All density functional theory (DFT) calculations were performed with the GPAW electronic structure code [34]. The wave functions are expanded on a real space grid with a grid spacing of 0.18 Å and we use the PBE exchange-correlation (xc)-functional [35]. All the pristine structures have been relaxed until the forces on each atom were below 0.05 eV/Å.

Structures with chalcogen vacancies were modelled using a 3×3 supercell, see Figure 1.

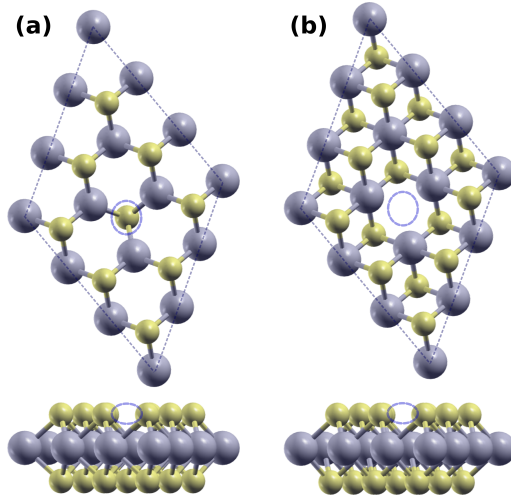


FIG. 1. (a) Top and sideview of a prototypical structure of a metal dichalcogenide in the 2H structure used for the defect calculations. The unit cell is shown by the dotted lines. The defect structure is created by making a chalcogen vacancy as indicated by a blue ellipse. (b) Similar figure as (a) for the 1T structure.

In this work we base our analysis of defect states on the PBE single-particle band structures. This may seem as a drastic oversimplification as the PBE is known to underestimate the band gap of semiconductors, and its description of localised states is also problematic due to self-interaction errors which tend to push occupied levels up in energy. However, due to the large number of systems investigated here, and because we are interested in the qualitative features of the band structure, i.e. whether or not the vacancies introduce localized states in the gap, rather than the absolute energies of band edges and gap states, we rely on the PBE band structures in the present work. As discussed below we find that the PBE results are qualitatively fully consistent with the more rigorous Slater-Janak theory.

The standard way to analyse defect energy levels in semi-conductors is based on total energy calculations for supercells containing the defect in different charge states. This procedure is, however, not straightforward. For example, it does not overcome the PBE band gap problem, and thus the correct band edge positions must be inferred from experiments or more accurate calculations such as the GW method. [36] Moreover, the slow convergence of the total energy of a charged supercell with the cell size implies that some kind of energy correction scheme must be applied to achieve meaningful numbers and there is no unique solution to this problem. [37–42] Alternatively, Slater-Janak (SJ) transition state theory

may be used to obtain the defect levels without the need to compare total energies of differently charged systems.[43, 44] The SJ method exploits that the Kohn-Sham eigenvalues are related to the derivative of the total energy E with respect to the occupation number η_i of the respective orbital,

$$\frac{\partial E[N]}{\partial \eta_i} = \varepsilon_i. \quad (1)$$

Assuming that the eigenvalue for the highest occupied state ε_H varies linearly with the occupation number (this is in fact a very good approximation), the electron affinity level can be obtained as

$$E^{N+1} - E^N = \int_0^1 \varepsilon_H(\eta) d\eta = \varepsilon_H\left(\frac{1}{2}\right). \quad (2)$$

Thus one obtains the electron affinity level (ionization potential) as the highest unoccupied (lowest occupied) single-particle eigenvalue of the system with 0.5 electron added to (removed from) the supercell. The SJ model has previously been shown to predict semiconductor defect levels in good agreement with the results obtained from more elaborate total energy difference schemes.[45]

For all 29 TMDs, we have applied the SJ method to compute the ionization potential and electron affinity levels of a 3×3 supercell containing a chalcogen vacancy. For consistency the systems have been structurally relaxed with the added ± 0.5 electron in the supercell. The results do not differ qualitatively from those derived from the PBE band structure of the neutral supercells. In particular, the two methods predict the same set of materials to be defect tolerant and defect sensitive, respectively. However, there are small differences between the two approaches. Taking MoS_2 as an example, the neutral PBE spectrum shows an occupied defect level positioned around 0.2 eV above the top of the valence band, see Fig. 2(a). After removal of 0.5 electron, the self-consistent PBE spectrum no longer shows this defect level. This indicates that the PBE description places the occupied defect level too high in energy which is most likely due to the PBE self-interaction error. Interestingly, PBE total energy difference calculations find the defect state below the valence band maximum in agreement with the SJ calculation.[22] However, this disagreement with the neutral PBE spectrum does not affect the conclusions regarding the defect tolerance of MoS_2 because both PBE and SJ consistently predict the presence of unoccupied defect levels at around 0.7 eV below the conduction band minimum (see Fig. 2(a)) which again agrees with calculations based on total energy differences.[22]

We mention that PBE+U calculations were also performed for all the TMDs with U values ranging from 0 to 4 eV. However, the band gaps of the group VI and group X TMDs were found to decrease with increasing U leading to unphysical small band gaps for common U values. Based on these findings, we do not consider PBE+U to be more accurate than PBE for the considered class of TMDs.

Figure 2 (a) shows the PBE band structures, the total density of states (DOS) and the projected density of states (PDOS) on the chalcogen p -orbitals and metal d -orbitals of 2H-MoS₂ in its pristine form (left) and with an S vacancy (right). The three narrow bands inside the band gap (one just above the valence band edge and two almost degenerate bands just above the band gap center) are formed by dangling Mo d bonds localized around the S vacancy. From the PDOS it is seen that the valence band maximum (VBM) and conduction band minimum (CBM) have very similar orbital character indicating that they consist of bonding and anti-bonding combinations of sulphur p and metal d states, respectively. We note that the finite size of the supercell (3×3) is responsible for the small dispersion of the deep gap states. We have found that applying a 4×4 supercell does not change the conclusions.

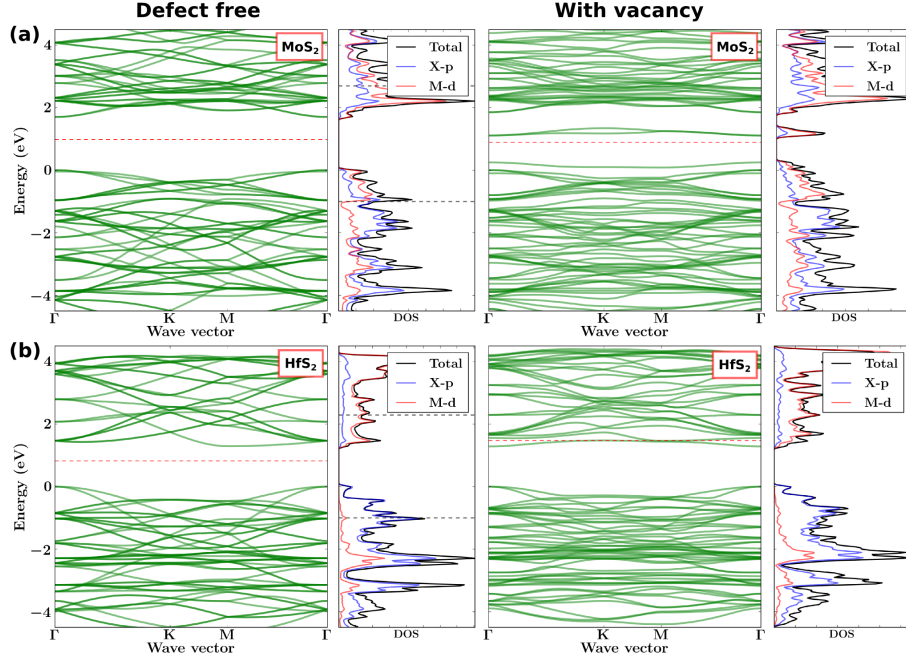


FIG. 2. (a)PBE band structures, the DOS and the PDOS on the chalcogen p -orbitals and metal d -orbitals of the monolayer 2H-MoS₂ in its pristine form (left) and and with an S vacancy (right). For comparison, the band structure is plotted for 3×3 supercell for the pristine as well as the defect structure. The energy levels have been aligned to the valence band maximum of the pristine monolayer. (b) Similar figure as (a) for 1T-HfS₂

Figure 2 (b) shows a similar plot as Figure 2 (a) for 1T-HfS₂. In contrast to MoS₂ this compound largely conserves its electronic structure around the band edges and no defect state is introduced. Additionally, the DOS plot shows that the states near the VBM are mostly dominated by the chalcogen p states whereas the CBM edge states mainly consist of the metal d states.

The above examples indicate that the orbital character of the valence/conduction bands are crucial for the tendency to form deep gap states. Based on the above picture the materials can be categorized in two classes; one with conduction and valence bands composed of bonding and anti-bonding combinations of similar orbitals, the other with valence and conduction bands composed of orbitals with distinctly different character, see Figure 3.

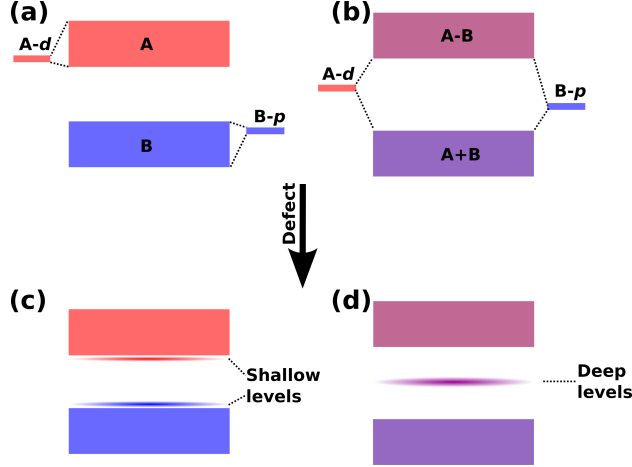


FIG. 3. (a) and (b) show the nature of the band structures near the band edges for the defect tolerant and defect sensitive cases respectively. In all the TMDs studied here, the states near the band edges primarily have contributions from the metal d states and chalcogen p states. In the defect tolerant case the nature of the bands near the band edges are significantly different whereas in the defect sensitive case they are of mixed nature. (c) and (d) show the shallow and deep levels introduced after the creation of defects.

This picture also agrees with previous works on defect tolerance in semiconductors. [46] The correspondence between the orbital character of the bands and the defect tolerance can be understood from elementary chemical bond theory. In the case of similar orbital character of the valence and conduction bands, the former will have bonding character and the latter will have the anti-bonding character. This implies that the energy of the individual orbitals should lie inside the band gap, see Figure 3 (b). Thus the creation of a vacancy leaves a dangling bond state corresponding to one of the orbitals lying deep in the band gap. On the other hand, different orbital character of the valence and conduction bands suggests that these bands are formed by orbitals lying outside the band gap, and therefore dangling bond states should not fall inside the gap. To quantify the orbital character of the electronic states in a given energy window from E_1 to E_2 we introduce the orbital fingerprint vector,

$$|\alpha\rangle = \frac{1}{\sqrt{c}} \begin{bmatrix} \rho_{\nu_1} \\ \rho_{\nu_2} \\ \vdots \\ \rho_{\nu_N} \end{bmatrix} \quad (3)$$

where c is a normalization constant, the ν_i 's are (a, l) pairs where 'a' and 'l' denote the atom

and angular momentum channel, respectively; and ρ_{ν_i} is the projected density of states onto the atomic orbital ϕ_{ν_i} integrated over the energy window,

$$\rho_{\nu_i} = \sum_n \int_{E_1}^{E_2} |\langle \psi_n | \phi_{\nu_i} \rangle|^2 \delta(E - E_n) dE \quad (4)$$

Using the orbital fingerprint vector we can define the normalized orbital overlap (NOO) between two manifolds of bands located in the energy windows E_1^v to E_2^v and E_1^c to E_2^c as

$$D = \langle \alpha | \beta \rangle \quad (5)$$

where α and β correspond to the valence and conduction band manifolds. By taking the two energy windows to lie around the VBM and CBM, respectively, we have a measure of the difference in average orbital character around the valence and conduction band edges. We note that $D = 0$ for materials with completely different character of the valence and conduction bands while $D = 1$ for materials with identical orbital character at the valence and conduction bands.

We have computed D (with an energy window of 1 eV above/below the conduction/valence band extrema) for a set of 29 monolayer TMDs, see Figure 4. We have carried out band structure calculations like the ones shown in Figure 2 for all 29 TMDs. For all the materials with $D \sim 1$ we find localized states inside the band gap. In contrast all the materials with D significantly less than 1 do not show deep gap states. The compounds exhibiting deep defect states after the removal of a chalcogen atom are shown with red circles in the Figure 4 whereas the compounds where no deep defect states are introduced after a chalcogen atom is removed are marked with green circles. This clearly shows that the normalized orbital overlap between the valence and conduction band manifolds represent a reliable and quantitative descriptor for the degree of defect tolerance of the TMDs. We stress that this rule should apply to the case of vacancies, crystal distortions, or other perturbations whose effect is to distort the intrinsic bonding. On the other hand, in the case of impurity atoms, the presence of deep gap states depends also on the energy of the atomic orbitals of the impurity atom relative to the band edges.

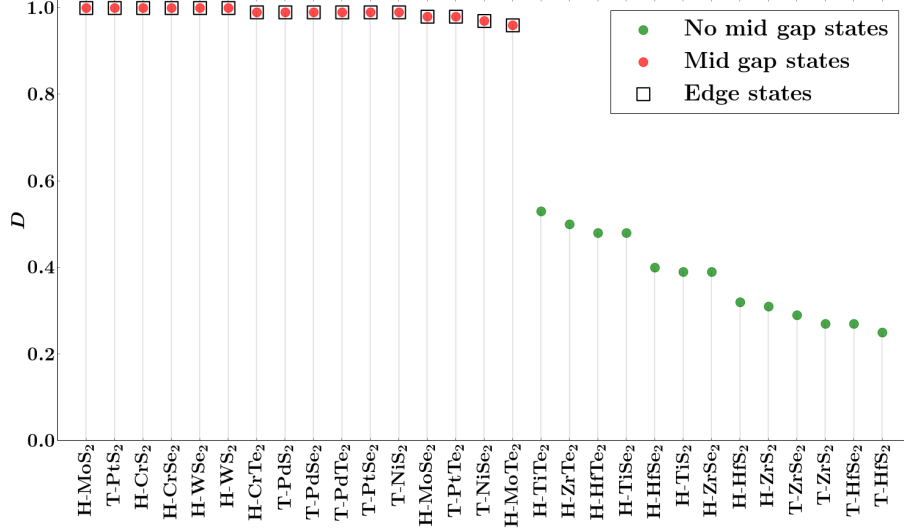


FIG. 4. The plot showing the compounds (y-axis) and the corresponding D values (x-axis). Red circles indicate the compounds manifesting deep defect states and the green circles indicating the compounds showing no deep defect states after the removal of a chalcogen atom. The black squares represent compounds showing states appearing deep in the band gap after cleaving the monolayer to form nanoribbons. Cr, Mo and W dichalcogenides are group-IV, Ti, Zr and Hf dichalcogenides are group-VI and Ni, Pd and Pt dichalcogenides are group-X.

A clear division of 29 TMDs into defect tolerant and defect sensitive materials can be understood from Figure 5. The splitting of the levels, the relative contribution of the chalcogen- p and metal- d and the position of the Fermi level decides the value of the descriptor. For example, in the 1T the position of the Fermi level in group-4 TMDs leads to the VBM having chalcogen- p and the CBM having metal- d character hence leading to defect tolerance. On the other hand, filling up of more levels in group-10 compounds places the Fermi level in such a way that the VBM and CBM states have dominant chalcogen- p character (for example, see SI for PDOS of NiS₂) resulting in similar orbital fingerprint vectors consequently leading to defect sensitivity. A similar argument can be applied to the compounds of group-6 in the 2H structure.

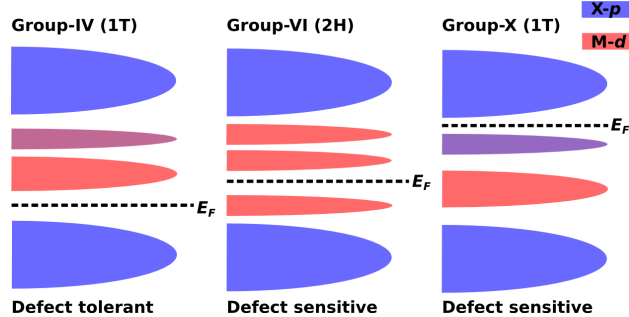


FIG. 5. The sketch showing the filling of the electronic levels of the different groups of the transition metal dichalcogenides. The TMDs of group-IV are defect tolerant whereas the TMDs of group-VI & X are defect sensitive. The chalcogen p states are shown in blue and the metal d states in red. The regions with mixed color have mixed p and d character.

Additionally, we also calculated the band structure of nanoribbons cleaved from the monolayer TMDs. As recently explained, TMD nanoribbons cleaved along a polar direction will manifest metallic edge states due to the presence of a dipole across the ribbon. [47] However, cleaving the monolayer along a non-polar direction can introduce edge states due to the formation of dangling bonds thus having a close resemblance to the case of a monolayer with a vacancy where the shallow/deep levels arise due to the presence of dangling bonds. Therefore, we expect that the arguments for the monolayers with vacancies will also be applicable for the edges in the nanoribbons.

Figure 6 (a) and (b) show the structure of the non-polar nanoribbons of the 2H and 1T structures, respectively, used for the analysis of the edge states. The edges of the nanoribbons are directed along the horizontal axis. In Figure 4 the nanoribbons supporting edge states (lying deep) in the band gap are shown with open squares. The figure consistently shows that only the defect sensitive TMDs form edge states deep in the band gap whereas the defect tolerant TMDs form only shallow, or no, edge states in the band gap. This indicates that the analysis based on the NOO descriptor is rather general and should be applicable to other system with imperfections involving dangling bonds. We are currently investigating the descriptor and possible generalizations of it for different classes of semiconductors.

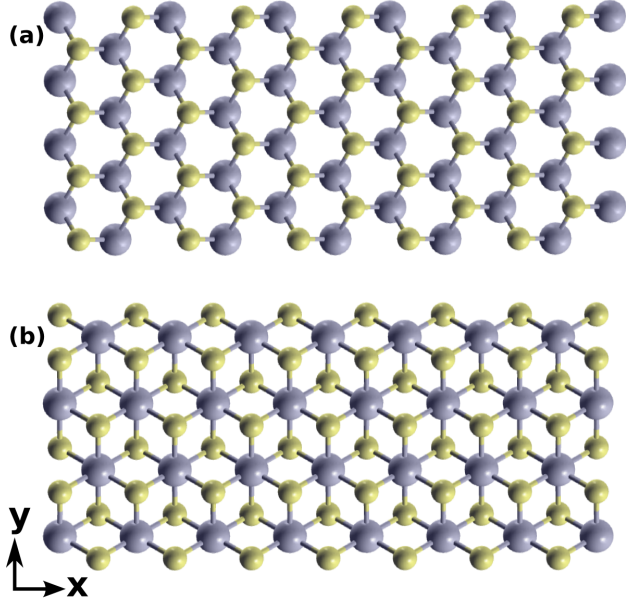


FIG. 6. (a) shows the structure of a nanoribbon of the 2H structure cleaved along the non-polar direction. The edges of the nanoribbons lie along the x-axis with a finite width along the y-axis; (b) shows a nanoribbon cleaved from the 1T structure.

In summary, we have explored the sensitivity of the band structure of 2D TMDs towards chalcogen vacancies. Our analysis shows that the tendency of the materials to form localized states within the band gap strongly depends on the similarity of the orbital character of the states near the conduction and valence band. These ideas were made quantitative by introducing a simple descriptor based on the projected density of states at the conduction and valence band edges. For a set of 29 semiconducting TMDs we found a clear correlation between the size of this descriptor and the presence of deep gap states induced by a chalcogen vacancy or by the formation of a one-dimensional edge. The idea of identifying defect tolerant materials based on a quantitative descriptor measuring valence and conduction band state similarity is completely general. In particular it does not depend on the dimensionality of the material, and should be useful both as general concept and as a tool for computational prediction of defect tolerant compounds.

ACKNOWLEDGMENTS

The authors acknowledge support from the Danish Council for Independent Research's Sapere Aude Program, Grant No. 11-1051390. The Center for Nanostructured Graphene is sponsored by the Danish National Research Foundation, Project DNRF58.

- [1] K. F. Mak, C. Lee, J. Hone, J. Shan, and T. F. Heinz, *Phys. Rev. Lett.* **105**, 136805 (2010)
- [2] A. Splendiani, L. Sun, Y. Zhang, T. Li, J. Kim, C.-Y. Chim, G. Galli, and F. Wang, *Nano Lett.* **10**, 1271 (2010)
- [3] H. Zeng, G.-B. Liu, J. Dai, Y. Yan, B. Zhu, R. He, L. Xie, S. Xu, X. Chen, W. Yao, and X. Cui, *Sci. Rep.* **3** (2013)
- [4] Y. Zhang, T.-R. Chang, B. Zhou, Y.-T. Cui, H. Yan, Z. Liu, F. Schmitt, J. Lee, R. Moore, Y. Chen, H. Lin, H.-T. Jeng, S.-K. Mo, Z. Hussain, A. Bansil, and Z.-X. Shen, *Nat. Nanotechnol.* **9**, 111 (2014)
- [5] T. Cao, G. Wang, W. Han, H. Ye, C. Zhu, J. Shi, Q. Niu, P. Tan, E. Wang, B. Liu, and J. Feng, *Nat. Commun.* **3**, 887 (2012)
- [6] K. F. Mak, K. He, J. Shan, and T. F. Heinz, *Nat. Nanotechnol.* **7**, 494 (2012)
- [7] K. Kaasbjerg, K. S. Thygesen, and K. W. Jacobsen, *Phys. Rev. B* **85**, 115317 (2012)
- [8] K. Kaasbjerg, K. S. Thygesen, and A.-P. Jauho, *Phys. Rev. B* **87**, 235312 (2013)
- [9] X. Cui, G.-H. Lee, Y. D. Kim, G. Arefe, P. Y. Huang, C.-H. Lee, D. A. Chenet, X. Zhang, L. Wang, F. Ye, and *et al*, *Nat. Nanotechnol.* **10**, 534 (2015)
- [10] L. Britnell, R. M. Ribeiro, A. Eckmann, R. Jalil, B. D. Belle, A. Mishchenko, Y.-J. Kim, R. V. Gorbachev, T. Georgiou, S. V. Morozov, A. N. Grigorenko, A. K. Geim, C. Casiraghi, A. H. C. Neto, and K. S. Novoselov, *Science* **340**, 1311 (2013)
- [11] M. Bernardi, M. Palumbo, and J. C. Grossman, *Nano Lett.* **13**, 3664 (2013)
- [12] H. J. Conley, B. Wang, J. I. Ziegler, R. F. Haglund, S. T. Pantelides, and K. I. Bolotin, *Nano Lett.* **13**, 3626 (2013)
- [13] Q. Liu, L. Li, Y. Li, Z. Gao, Z. Chen, and J. Lu, *J. Phys. Chem. C* **116**, 21556 (2012)
- [14] H. Rostami, A. G. Moghaddam, and R. Asgari, *Phys. Rev. B* **88**, 085440 (2013)
- [15] G. Gao, W. Gao, E. Cannuccia, J. Taha-Tijerina, L. Balicas, A. Mathkar, T. N. Narayanan,

- Z. Liu, B. K. Gupta, J. Peng, Y. Yin, A. Rubio, and P. M. Ajayan, *Nano Lett.* **12**, 3518 (2012)
- [16] A. K. Geim and I. V. Grigorieva, *Nature* **499**, 419 (2013)
- [17] K. Andersen, S. Latini, and K. S. Thygesen, *Nano Lett.* **15**, 4616 (2015)
- [18] M. Chhowalla, H. S. Shin, G. Eda, L.-J. Li, K. P. Loh, and H. Zhang, *Nat. Chem.* **5**, 263 (2013)
- [19] X. Wen, Y. Feng, S. Huang, F. Huang, Y.-B. Cheng, M. Green, and A. Ho-Baillie, *J. Mater. Chem. C* **4**, 793 (2016)
- [20] S. McDonnell, R. Addou, C. Buie, R. M. Wallace, and C. L. Hinkle, *ACS Nano* **8**, 2880 (2014)
- [21] H. Qiu, T. Xu, Z. Wang, W. Ren, H. Nan, Z. Ni, Q. Chen, S. Yuan, F. Miao, F. Song, G. Long, Y. Shi, L. Sun, J. Wang, and X. Wang, *Nat. Commun.* **4**, 2642 (2013)
- [22] H.-P. Komsa and A. V. Krashenninikov, *Phys. Rev. B* **91**, 125304 (2015)
- [23] H. Wang, C. Zhang, and F. Rana, *Nano Letters* **15**, 339 (2015)
- [24] O. Lopez-Sanchez, D. Lembke, M. Kayci, A. Radenovic, and A. Kis, *Nat. Nanotechnol.* **8**, 497 (2013)
- [25] J. S. Ross, P. Klement, A. M. Jones, N. J. Ghimire, J. Yan, D. G. Mandrus, T. Taniguchi, K. Watanabe, K. Kitamura, W. Yao, D. H. Cobden, and X. Xu, *Nat. Nanotechnol.* **9**, 268 (2014)
- [26] J. Lu, A. Carvalho, X. K. Chan, H. Liu, B. Liu, E. S. Tok, K. P. Loh, A. H. C. Neto, and C. H. Sow, *Nano Lett.* **15**, 3524 (2015)
- [27] M. Amani, D.-H. Lien, D. Kiriya, J. Xiao, A. Azcatl, J. Noh, S. R. Madhupathy, R. Addou, S. KC, M. Dubey, K. Cho, and et al., *Science* **350**, 1065 (2015)
- [28] J. Suh, T.-E. Park, D.-Y. Lin, D. Fu, J. Park, H. J. Jung, Y. Chen, C. Ko, C. Jang, Y. Sun, R. Sinclair, J. Chang, S. Tongay, and J. Wu, *Nano Lett.* **14**, 6976 (2014)
- [29] H. Wan, L. Xu, W.-Q. Huang, J.-H. Zhou, C.-N. He, X. Li, G.-F. Huang, P. Peng, and Z.-G. Zhou, *RSC Adv.* **5**, 7944 (2015)
- [30] C. Chakraborty, L. Kinnischtzke, K. M. Goodfellow, R. Beams, and A. N. Vamivakas, *Nat. Nanotechnol.* **10**, 507 (2015)
- [31] T. T. Tran, K. Bray, M. J. Ford, M. Toth, and I. Aharonovich, *Nat. Nanotechnol.* **11**, 37 (2016)
- [32] H. Li, C. Tsai, A. L. Koh, L. Cai, A. W. Contryman, A. H. Fragapane, J. Zhao, H. S. Han, H. C. Manoharan, F. A.-Pedersen, J. K. Nørskov, and X. Zheng, *Nat. Mater.* **15**, 48 (2016)

- [33] F. A. Rasmussen and K. S. Thygesen, *J. Phys. Chem. C* **119**, 13169 (2015)
- [34] J. Enkovaara, C. Rostgaard, J. J. Mortensen, J. Chen, M. Dułak, L. Ferrighi, J. Gavnholt, C. Glinsvad, V. Haikola, H. A. Hansen, and *et al*, *J. Phys.: Condens. Matter* **22**, 253202 (2010)
- [35] J. P. Perdew, K. Burke, and M. Ernzerhof, *Phys. Rev. Lett.* **77**, 3865 (1996)
- [36] F. Huser, T. Olsen, and K. S. Thygesen, *Phys. Rev. B* **88**, 245309 (2013)
- [37] M. Leslie and N. J. Gillan, *Journal of Physics C: Solid State Physics* **18**, 973 (1985)
- [38] G. Makov and M. C. Payne, *Phys. Rev. B* **51**, 4014 (1995)
- [39] S. Lany and A. Zunger, *Phys. Rev. B* **78**, 235104 (2008)
- [40] C. Freysoldt, J. Neugebauer, and C. G. Van de Walle, *Phys. Rev. Lett.* **102**, 016402 (2009)
- [41] H.-P. Komsa, T. T. Rantala, and A. Pasquarello, *Phys. Rev. B* **86**, 045112 (2012)
- [42] P. A. Schultz, *Phys. Rev. Lett.* **84**, 1942 (2000)
- [43] F. Gallino, G. Pacchioni, and C. Di Valentin, *J. Chem. Phys.* **133**, 144512 (2010)
- [44] A. Chakrabarty and C. H. Patterson, *J. Chem. Phys.* **137**, 054709 (2012)
- [45] Y. Li, S. Sanna, and W. G. Schmidt, *J. Chem. Phys.* **140**, 234113 (2014)
- [46] A. Zakutayev, C. M. Caskey, A. N. Fioretti, D. S. Ginley, J. Vidal, V. Stevanovic, E. Tea, and S. Lany, *J. Phys. Chem. Lett.* **5**, 1117 (2014)
- [47] M. Gibertini and N. Marzari, *Nano Lett.* **15**, 6229 (2015)